

UDK 549.632; 622.785

## The Influence of Compaction Pressure on the Density and Electrical Properties of Cordierite-based Ceramics

N. Obradović<sup>1,\*</sup>), N. Đorđević<sup>2</sup>, A. Peleš<sup>1</sup>, S. Filipović<sup>1</sup>, M. Mitrić<sup>3</sup>,  
V. B. Pavlović<sup>1</sup>

<sup>1</sup>Institute of Technical Sciences of SASA, Knez Mihajlova 35/IV, 11000 Belgrade, Serbia

<sup>2</sup>Institute for Technology of Nuclear and Other Mineral Raw Materials, Bulevar Franse d'Eperea 86, 11000 Belgrade, Serbia

<sup>3</sup>Vinča Institute of Nuclear Sciences, University of Belgrade, Mike Alasa 12-14, 11000 Belgrade, Serbia

---

### Abstract:

*Due to its characteristics, cordierite,  $2\text{MgO}\cdot 2\text{Al}_2\text{O}_3\cdot 5\text{SiO}_2$ , is a high-temperature ceramic material of a great scientific interest. Mechanical activation of the starting mixtures containing 5.00 mass%  $\text{TiO}_2$  was performed in a high-energy ball mill for 10 minutes. The compaction pressure varied from 0.5 to  $6\text{tcm}^{-2}$  (49–588 MPa). The sintering process was performed at 1350°C for four hours in the air atmosphere. The phase composition of the activated and sintered samples was analyzed using X-ray diffraction. Scanning electron microscopy was used to analyze the microstructure of both compacted and sintered samples. The authors have investigated the influence of compaction pressure on the sintered samples and their electrical properties.*

**Keywords:** Mechanical activation, Density, XRD, SEM, Electrical properties, Cordierite.

---

## 1. Introduction

Cordierite-based ceramics, with the basic chemical composition of  $2\text{MgO}\cdot 2\text{Al}_2\text{O}_3\cdot 5\text{SiO}_2$ , are widely used in various fields, from substrates for micro-electronic packaging industry to cookware, heat exchangers, glazes for floor tiles, etc. Owing to its low-temperature thermal expansion coefficient ( $20\cdot 10^{-7}\text{°C}^{-1}$ ) and low relative dielectric constant ( $\sim 5$ ), these ceramic materials are also well-known by their good thermo-mechanical, chemical and dielectric properties [1,2]. Therefore, these could be applicable as materials exposed to sudden temperature changes [3-7] and also as semiconducting bearers [8,9].

Our previous studies [10] show that the mechanical activation of starting components (kaolin, quartz, magnesium oxide) has a significant impact on the lowering of the sintering temperature. It has been demonstrated that, compared to non-activated components, mechanically activated ones increase energy due to induced crystal defects. During a mechanochemical treatment, several processes occur: attrition of the starting material, crystal lattice destruction, the formation of various defects, etc. All of the mentioned processes increase the chance for reactions to occur at temperatures lower than usual [11]. Furthermore, mechanical activation could affect the final electrical characteristics; accordingly, it is very

---

\*) Corresponding author: obradovic.nina@yahoo.com

important to take into account and understand the changes that are introduced into the system during milling.

The application of compaction pressure is an unavoidable technological procedure in the sintering process [12-15]. The importance of this procedure is obvious, having in mind that pressure conditions have an influence on intergranular contacts, which play an important role in the sintering process. The initial density of samples is one of the essential parameters and it has an important role in the final characterization of the microstructure. Along with the applied pressure, the packing of powder particles is also the function of the material's class, the shape of primary particles and the strenght of interparticle connections, etc. [13,16].

In this paper, the authors have investigated the influence of compaction pressure on the density and the microstructure of mechanically activated powders as well as the density and electrical properties of the sintered samples.

## 2. Experimental procedure

In these experiments, authors used Mg(OH)<sub>2</sub>, Al<sub>2</sub>O<sub>3</sub>, SiO<sub>2</sub> and TiO<sub>2</sub> (all p.a. purity). The mixture of MgO+Al<sub>2</sub>O<sub>3</sub>+SiO<sub>2</sub> in the 2:2:5 ratio, with the addition of 5.00 mass% TiO<sub>2</sub>, was mechanically activated by grinding in a high-energy planetary ball mill. ZrO<sub>2</sub> vessels and balls with the powder-to-balls mass ratio of 1:40 were used. The milling process was performed in the air atmosphere for 10 minutes. The samples were denoted as K-10, according to the milling time. The X-ray powder diffraction patterns after milling and sintering were obtained using a Philips PW-1050 diffractometer with λCu-K<sub>α</sub> radiation and a step/time scan mode of 0.05° 1s<sup>-1</sup>. The morphology of the obtained powders and sintered samples was characterized by scanning electron microscopy (JEOL JSM-6390 LV). The powders were crushed and covered with gold in order to perform these measurements.

The pressure used in our experiments was 0.5–6 tcm<sup>-2</sup> (49–588 MPa). The amount of the samples was 0.30 g. The pressure was performed in a double-sided tool 6 mm in diameter (Hydraulic press RING 14, VEB THURINGER). The density of the specimens was calculated from the measurements of their diameter, thickness, and mass. The theoretical density (TD) of the mixture was 3.078 gcm<sup>-3</sup> and was calculated based using the following equation:

$$\rho_{mixture} = \frac{m_{mixture}}{V_1 + V_2 + V_3 + V_4} \quad (1)$$

where: m is the mass of the mixture (30.00 g), V<sub>1</sub>, V<sub>2</sub>, V<sub>3</sub> and V<sub>4</sub> are the volumes of Component 1 – MgO, Component 2 – SiO<sub>2</sub>, Component 3 – Al<sub>2</sub>O<sub>3</sub> and Component 4 – TiO<sub>2</sub> in the mixture, respectively, calculated using the TD of the components.

The compacts were placed in an alumina boat and heated in a tube furnace (Lenton Thermal Design Typ 1600), and then sintered isothermally at 1350°C in air atmosphere for four hours; the heating rate was 10°Cmin<sup>-1</sup>.

The electrical properties of the sintered samples were measured on 4262A LCR meter Hewlett Packard apparatus, at the frequency of 10 kHz.

## 3. Results and discussion

The results obtained after compaction are presented at Tab. I and Fig. 1. The density values were increased with the applied pressure and the greatest density was obtained after the compaction process at 6tcm<sup>-2</sup>.

**Tab. I** Density of green bodies obtained during the compaction of the cordierite powder with the addition of TiO<sub>2</sub> activated for 10 minutes.

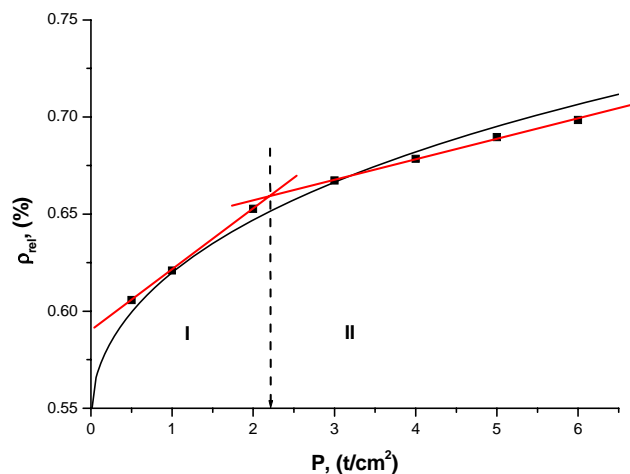
P (tcm <sup>-2</sup> )	ρ (gcm <sup>-3</sup> )	TD (%)	ρ <sub>rel</sub> (%)	Π
0.5	1.8647	60.58	0.6058	0.3942
1	1.9110	62.09	0.6209	0.3791
2	2.0090	65.27	0.6527	0.3473
3	2.0540	66.73	0.6673	0.3327
4	2.0885	67.85	0.6785	0.3215
5	2.1227	68.96	0.6896	0.3104
6	2.1500	69.85	0.6985	0.3015

P – compaction pressure, ρ – green-body densities, TD – sample density as percentage of the theoretical density, ρ<sub>rel</sub> – relative density, Π – sample porosity, (1-ρ<sub>rel</sub>)

The R. Panelli and F. Ambrozio Filho [17] equation is used in order to fit the obtained density values:

$$\ln\left(\frac{1}{1-D}\right) = AP^{\frac{1}{2}} + B \quad (2)$$

where: P is compaction pressure, D is the relative density, A is the parameter showing the powder's ability for compaction by plastic deformation and B is the parameter related to the density before compaction. The values of parameters A and B, obtained by fitting the experimental data using the Table Curve programme package are: A - 0.1785 and B - 0.7888.

**Fig. 1.** Relative density values as a function of pressure fitted (black curve) by the Panelli-Ambrozio Filho equation [17].

The authors of the compaction equation [17] state that parameter A (the slope of the curve) determines the plastic deformation ability of a powder. The higher the A parameter, the greater is deformation within the powder. Parameter B is a y-axis intercept, or the density of the powder with no pressure applied. Plastic materials have higher values of A, while brittle materials have lower A values. If we compare the results obtained in our previous studies [18] for other materials, such as oxides of Zn, Ti, Mg, we may conclude that this powder shows plastic deformation. However, if we take into account the complexity of this four-component system, the inability of the equation to fit complex systems and the fact that fitting results are not satisfactory, we can divide our results in two categories (two lines in Fig. 1). The first (I) covers the first phase of three pressures (0.5, 1 and 2tcm<sup>-2</sup>), while the second (II) extends over

the second phase ( $3 - 6\text{tcm}^{-2}$ ). The intersection of these two straight lines should clearly represent the distinction of two mechanisms to whose agency the powders are exposed during the compaction process. The first one is assigned to rearranging due to particles' mutual rapprochement and the second is the deformation breaking of powder particles [19].

The diffraction pattern for the K-10 mixture showed the presence of the starting components ( $\text{Mg}(\text{OH})_2$ ,  $\text{SiO}_2$ ,  $\text{Al}_2\text{O}_3$ ,  $\text{AlO}(\text{OH})$  and  $\text{TiO}_2$ ) [10]. Most peak intensities decreased during a 10-minute activation process, while some peaks were broadened, which indicated that processes of crystal lattice destruction, along with the amorphization, have started. This is in accordance with the results obtained after the calculations of microstructure parameters based on the approximation method. The crystallite size, calculated using Scherrer's equation, decreased from 63 to 48 nm for alumina, from 76 to 57 nm for silica, from 55 to 47 nm for titanium and from 53 to 46 nm for magnesium, during a 10-minute activation process.

Fig. 2. shows the SEM micrographs of the cordierite powder activated for 10 minutes and pressed under a) 0.5, b) 3 and c) 6  $\text{t/cm}^2$ .

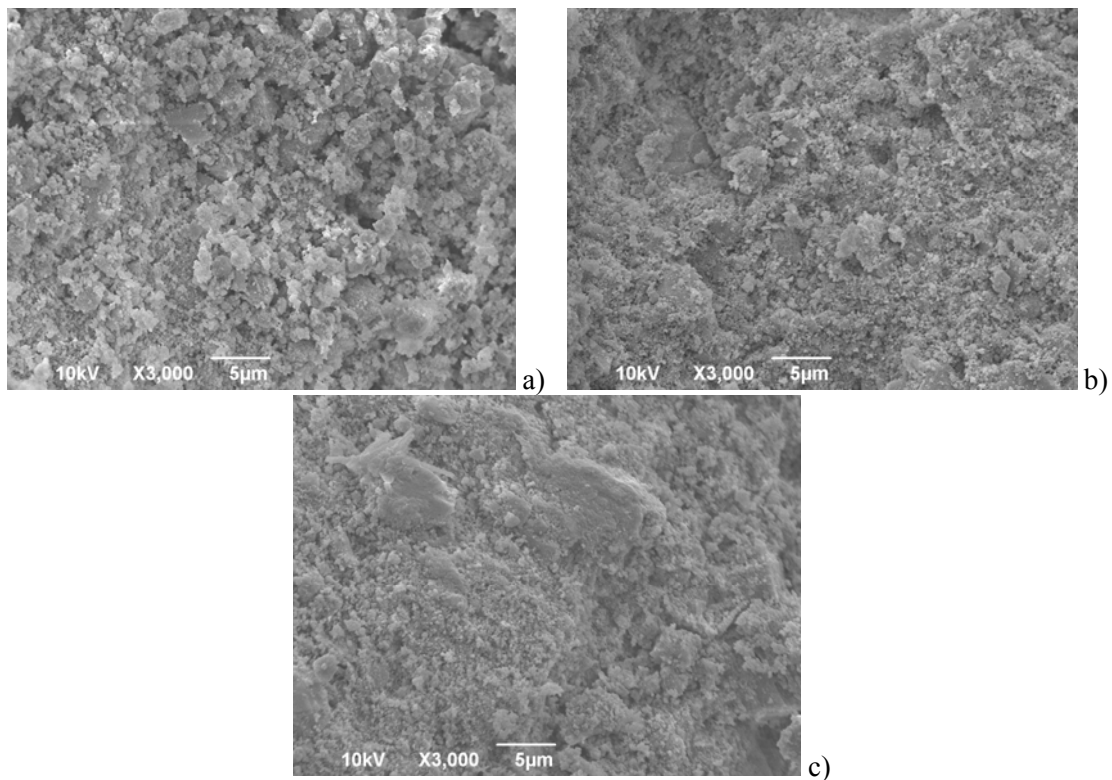


**Fig. 2.** SEM images of the starting cordierite powder pressed under a) 0.5, b) 3 and c) 6  $\text{t/cm}^2$ .

The powder pressed under  $0.5\text{tcm}^{-2}$  shows considerably high porosity and great voids between particles are noticeable. Powder particles are clearly defined and the surface on compact breaks is rough. With the increased pressure, powder particles are getting closer and defined agglomerates can be observed. It is clearly visible that samples pressed under  $6\text{tcm}^{-2}$  have a denser structure and an increased number of mutual contacts. The porosity also decreases and the shape of single particles is not so visible; it is right to say that blocks of agglomerates are formed, due to higher pressures.

Fig. 3. shows the SEM micrographs of the compacts pressed under a) 0.5, b) 3 and c) 6  $\text{tcm}^{-2}$  pressure, sintered at  $1350^\circ\text{C}$  for four hours. According to the presented SEM micrographs, we have obtained the expected results regarding the microstructure of the

sintered samples. Fig. 3. a) shows a small-grain structure with an open porosity. The sintered samples pressed under the pressure higher than  $2\text{tcm}^{-2}$  show the greatest change in microstructures, which is in accordance with Fig. 1.

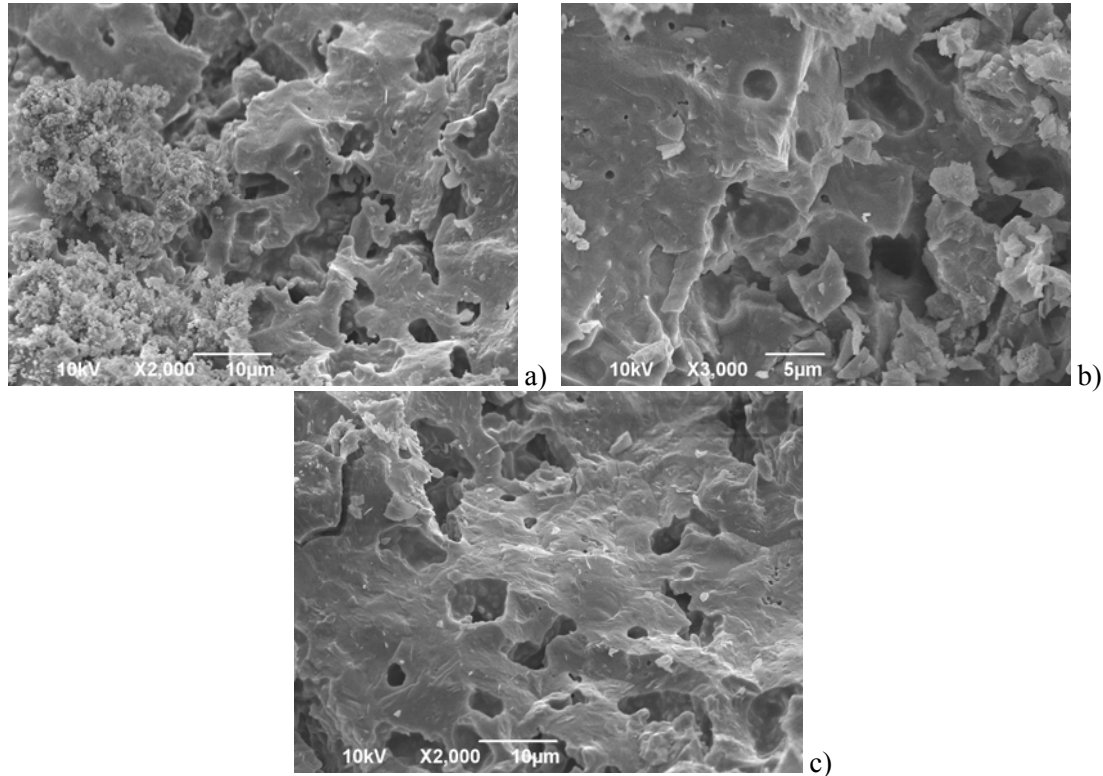


**Fig. 3.** SEM images of the compacts obtained under a) 0.5, b) 3 and c) 6  $\text{t/cm}^2$  pressure, sintered at  $1350^\circ\text{C}$  for 4h.

The absence of the small-grain structure in the samples compacted at pressures higher than  $2\text{tcm}^{-2}$  indicates that this pressure is the critical pressure that enables better contacts between particles. Fig. 3. c) shows a stable structure with large surfaces and a closed porosity, typical of the final sintering stage, which is the obvious effect of the pressure applied prior to the sintering process. Higher pressures allow for a great number of contacts between particles, leading to more compact samples without the small-grain structure.

Fig. 4. shows the XRD patterns of the samples pressed under a)  $0.5\text{tcm}^{-2}$  and b)  $6\text{tcm}^{-2}$ , both sintered at  $1350^\circ\text{C}$  for four hours. The obtained peaks were identified using JCPDS cards (084-1220 for cordierite, 074-2220 for  $\text{Mg}(\text{OH})_2$ , 083-2241 for  $\text{TiO}_2$  rutile, 074-0201 for  $\text{SiO}_2$ , 035-0310 for  $(\text{MgAl})\text{SiO}_3$ ). The XRD pattern shown in Fig. 4. a) indicates the existence of a cordierite phase along with some amount of un-reacted starting components, such as  $\text{SiO}_2$  and  $\text{Mg}(\text{OH})_2$ . The presence of a rutile phase has been expected, because it was added not with the idea of incorporating it into the cordierite crystal lattice but with the intention to influence the mechanical and electrical properties. Accompanied with the sintering process, the pressure of  $6\text{tcm}^{-2}$  yielded different phase compositions, as shown in Fig. 4. b). Apart from cordierite, as the major phase, no starting components (except  $\text{TiO}_2$ -rutile) have been detected. However, a  $(\text{MgAl})\text{SiO}_3$  phase is observed as a result of a reaction between the starting components,  $\text{Mg}(\text{OH})_2$  and  $\text{SiO}_2$ .

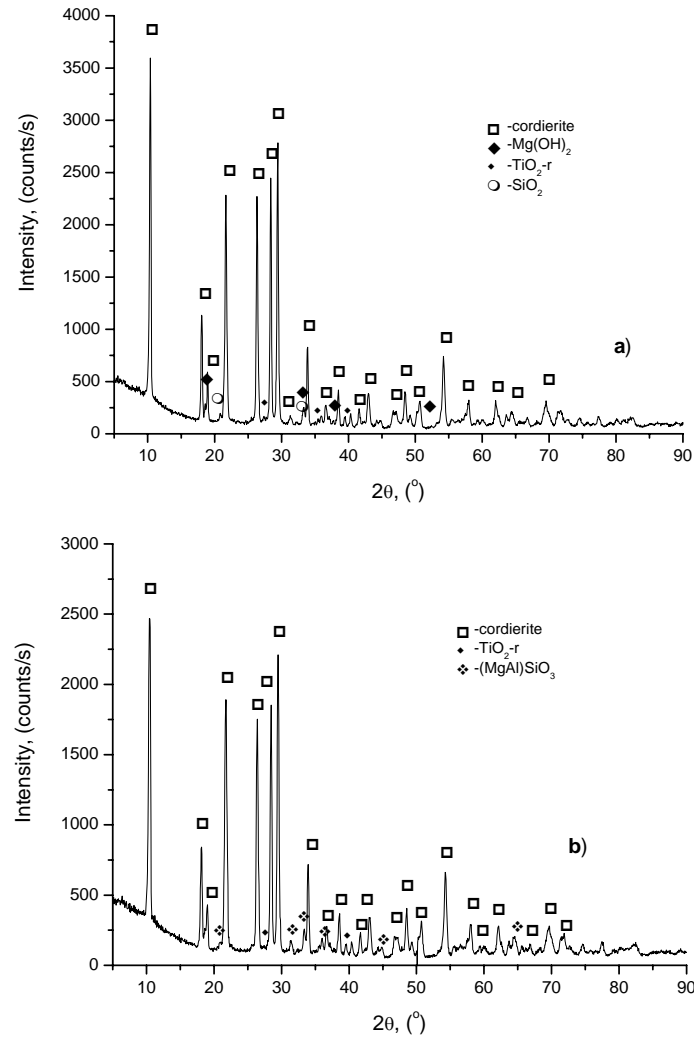


**Fig. 4.** XRD patterns of the samples compacted at a) 0.5 and b) 6t/cm<sup>2</sup> pressure, sintered at 1350°C for 4h.

The density after the sintering process at 1350°C for four hours, as well as with the electrical properties of cordierite ceramics are presented in Tab. II.

**Tab. II** Density and electrical properties of cordierite after sintering at 1350°C for four hours.

P (tcm <sup>-2</sup> )	C (pF)	tgδ	R (Ω)	ρ (gcm <sup>-3</sup> )	TG (%)	ε <sub>r</sub>
0.5	1.89	0.009	2·10 <sup>13</sup>	2.041	66.31	14.16
1	1.79	0.009	3·10 <sup>13</sup>	2.075	67.41	13.21
2	1.81	0.010	2·10 <sup>13</sup>	2.119	68.83	12.75
3	2.23	0.008	3·10 <sup>13</sup>	2.154	69.98	15.21
4	2.10	0.008	2·10 <sup>13</sup>	2.175	70.66	13.86
5	2.09	0.008	3·10 <sup>13</sup>	2.192	71.21	13.53
6	2.09	0.007	1·10 <sup>12</sup>	2.214	71.91	13.31

The electrical measurements are in a great accordance with the results presented earlier in this paper. It is obvious that they vary with the applied pressure. Two areas are visible: the first between 0.5 and 2  $\text{tcm}^{-2}$ , and the second between 3 and 6  $\text{tcm}^{-2}$  (parts I and II in Fig. 1). The values of the relative dielectric constant  $\epsilon_r$  are increased, compared to the normal value for cordierite ceramics, due to the addition of  $\text{TiO}_2$  and they vary in the interval from 13 to 15. Although the  $\epsilon_r$  value is increased, it is still in the acceptable dielectric range.

#### 4. Conclusions

The results of this study show that the applied pressure has an impact on the final characteristics of the sintered material:

- The density values of green bodies increase with the greater pressure applied and the greatest density is achieved after the compaction process at 6  $\text{tcm}^{-2}$ . Two stages are visible and the interval is between 2 and 3  $\text{tcm}^{-2}$ , indicating that powder particles are exposed to the agency of different mechanisms.
- The SEM micrographs clearly indicate a completely different microstructure: an open porosity and defined small-grain areas are observed in the powders pressed under lower pressures. With increased pressure values, a closed porosity and more homogeneous microstructures are obtained.
- According to the results presented in this study, the XRD analysis has shown a different phase composition in the sintered samples pressed under two limit pressures. The cordierite phase is the dominant phase; the starting components are present in the sample pressed under 0.5  $\text{tcm}^{-2}$ , whereas they were completely used in the reaction yielding a new phase in the sample pressed under 6  $\text{tcm}^{-2}$ .
- The final electrical properties are in great agreement with the presented results. The values of the relative dielectric constant show that the pressure of 2  $\text{tcm}^{-2}$  yields the results closest to the expected results; they are also consistent with standard demands related to the applicability of cordierite ceramics.

Based upon these results, we recommend compaction between 2 and 3  $\text{tcm}^{-2}$  as a phase preceding the sintering process because it ensures the most favorable phase composition, microstructure and electrical properties for this ceramic material.

#### 5. References

1. A. I. Kingon, R. F. Davis, Engineer Materials Handbook, Vol. 2. "Ceramics" edited by S. J. Schneider, Jr., ASM International Metals Park, OH, p. 1191.
2. N. Obradovic, N. Djordjevic, S. Filipovic, N. Nikolic, D. Kosanovic, M. Mitric, S. Markovic, V. Pavlovic, Powder Technology 218 (2012) 157-161.
3. V.J. Powers, C.H. Drummond, Ceram. Eng. Sci. Proc. 7 (1986) 969.
4. I. Warsworth, R. Stevens, J. Eur. Ceram. Soc. 9 (1992) 153.
5. M. Pinero, M. Atik, J. Zarzycki, J. Non-Cryst. Solids 147–148 (1992) 1523.
6. D. Kervadec, M. Coster, J.L. Chermant, Mater. Res. Bull 27 (1992) 967.
7. N. Clausen, G. Petzow, J. Phys. (Paris), 47 (1986) 693.
8. R. R. Tumala, J. Am. Ceram. Soc. 74 (1991) 895.
9. S. H. Knickerbocker, A. H.Kumar, L. W. Herron Am. Ceram. Soc. Bull. 72 (1993) 90.
10. N. Djordjevic, N. Obradovic, S. Filipovic, J. Zivojinovic, M. Mitric, S. Markovic, Tehnika – Novi materijali 21 (2012) 3, 329.

11. N. Đorđević, M.M. Ristić, Lj. Pavlović, M. Lazić, J. Stojanović, TEOTES, IV konferencija "Teorija i tehnologija sinterovanja" (2001) 25.
12. J. S. Reed, Introduction to the Principles of Ceramic Processing, Wiley, New York (1988) 158.
13. G. L. Messing, C. J. Markhoff, L. G. McCoy, J. Am. Ceram. Soc., 61 (1982) 857.
14. I. Shapiro, Adv. Powder Metall. Part. Mater., 3 (1994) 41.
15. J. K. Beddow, Particulate Science and Technology, Chemical Publishing Co., Inc. New York, (1980), 285.
16. R. M. German, Particle Packing Characteristics, Metal Powder Industries Federation, Princeton, New Jersey, (1989) 59.
17. R. Panelli, F. A. Filho, Powder Tech., 114 (2001) 255.
18. N. Obradovic, S. Stevanovic, M. Mitric, M. V. Nikolic, M. M. Ristic, Science of Sintering, 39 (2007) 241.
19. A. R. Cooper, L. E. Eaton, J. Amer. Ceram. Soc., 45 (1962) 97.

---

**Садржај:** Обзиром на својства, кордијерит,  $2\text{MgO}\cdot 2\text{Al}_2\text{O}_3\cdot 5\text{SiO}_2$ , је високо температурски керамички материјал од великог интереса за научнике. Почетна смеша са додатком 5,00 масених %  $\text{TiO}_2$  је активирана у високо енергетском млину, 10 минута. Притисак пресовања кје био у интервалу од 0,5 до 6  $\text{tcm}^{-2}$  (49–588 МПа). Извршено је синтеровање испресака на 1350 °С током 4 сата у атмосфери ваздуха. Фазни састав активираних и синтерованих узорака извршен је помоћу рендгенске дифракције. Скенирајућом електронском микроскопијом анализирани су микроструктуре. Аутори су испитивали утицај притиска пресовања на синтеровање и електрична својства кордијерита.

**Кључне речи:** механичка активација, густина, XRD, SEM, електрична својства, кордијерит.

---